Journal of
Applied Remote Sensing

Post-processing analysis of MODIS leaf area index subsets

Judith Horn
Karsten Schulz

SPIE

Downloaded from SPIE Digital Library on 18 Jan 2011 to 128.219.49.8. Terms of Use: http://spiedl.org/terms

Post-processing analysis of MODIS leaf area index subsets

Judith Horn[a] and Karsten Schulz[b]

Ludwig-Maximilians-Universität München, Department of Geography, Luisenstrasse 37
Munich, 80333 Germany
[a]judith horn@email.de
[b]k.schulz@lmu.de

Abstract. The global network FLUXNET supplies environmental scientists with valuable data on ecosystem exchange processes along with meteorological measurements. Ecosystem characteristics at these sites can be efficiently complemented by remote sensing data from the MODIS sensors on-board the NASA satellites Terra and Aqua. The ORNL DAAC makes resampled MODIS key products as so called 'Land Product Subsets' available. These subsets comprise selected MODIS products in a 7x7 km grid centered on FLUXNET sites. One of these products is the leaf area index (LAI). Despite the frequent application of MODIS LAI data in ecosystem models, there is still no consensus on its usage and the employment of the additionally provided quality criteria (QC). In this study, we analyze the effects of various QC filters, spatial aggregations and sensor choices on magnitude and temporal dynamics of LAI data at six FLUXNET sites. Additionally, we assess the sensitivity of a simple soil-vegetation-atmosphere-transfer (SVAT) model on differently post-processed LAI times series. It is found that it is advantageous to combine the products of both sensors. The consideration of quality assessments is essential, but the QC application is not straightforward for forest sites and the QC choice can have significant effects on the resulting LAI time series with considerable consequences on the outcome of subsequently applied SVAT models.

Keywords: Leaf area index, MODIS, SVAT, quality criteria, latent heat flux

1 INTRODUCTION

Continuous eddy covariance measurements by micro-meteorological flux towers have become indispensable in monitoring the exchange of energy, carbon and water fluxes between the terrestrial surface and the atmosphere. The global network FLUXNET [1] merges these valuable data collected around the world in a comprehensive database and provides the scientific community an unique opportunity to establish understanding of ecosystem exchange processes and set up, calibrate and validate models to predict ecosystem behavior in a changing environment [2, 3].

However, flux towers can only catch a glimpse on ecosystem processes given their point measurement nature which stands in contrast to the usually more extensive, spatially continuous model application scale. Satellite remote sensing, instead, offers spatially continuous information and can consequently help to dissolve the dilemma of having scattered point measurements on the one hand and the need to analyze and predict exchange processes at a local, regional or even global scale on the other hand by bridging the gap between these scales [4, 5]. Furthermore, remote sensing can provide ecosystem characteristics that are time-consuming or difficult to gather in the field [6]. Vice versa, the validation of remote sensing products relies on continuous measurements such as done at the FLUXNET sites [7, 8].

The MODIS sensor on-board the satellites Terra and Aqua launched within the framework of NASA's EOS program (Earth Observing System) has proven itself a key sensor in remote sensing of ecosystem dynamics and land surface processes [9]. In this respect, MODIS data have

©2010 Society of Photo-Optical Instrumentation Engineers [DOI: 10.1117/1.3524265]
Received 17 Mar 2010; accepted 3 Nov 2010; published 15 Nov 2010 [CCC: 19313195/2010/$25.00]

Downloaded from SPIE Digital Library on 18 Jan 2011 to 128.219.49.8. Terms of Use: http://spiedl.org/terms

been widely applied in studies to detect the vegetation physiological status [10, 11]. The synergetic interaction between micro-meteorological tower measurements, modeling and remote sensing is supported by the Oak Ridge National Laboratory Distributed Active Archive Center (ORNL DAAC): This institute makes resampled key remote sensing products from MODIS (Moderate Resolution Imaging Spectroradiometer) as so called 'MODIS Land Product Subsets' freely available. These files are provided in an easy to handle ascii-format and comprise selected MODIS land products in a 7x7 km grid centered on FLUXNET and other field measurement sites. One of these subset products retrieved by radiative transfer modeling with MODIS Terra and Aqua data is 'MOD15A2' or 'MYD15A2', respectively, which provides 8-day estimates of the leaf area index (LAI $[m^2 m^{-2}]$) accompanied by the closely related FPAR (Fraction of Absorbed Photosynthetically Active Radiation) [12].

The dimensionless LAI defined as one-sided surface area of leaves and needles per ground area [13, 14] is a main biophysical driver in ecosystem models [15–17]. The MODIS LAI product is also increasingly frequently used in applications such as numerical weather forecasting or hydrological modeling [18, 19]. The MODIS algorithm to retrieve the LAI is based on inverse radiative transfer modeling; in case of its failure under unfavorable conditions, an empirical back-up algorithm is triggered [20]. Quality criteria provide information about the suitability of the individual retrieval with respect to the algorithm path, the detector state, geometry problems and cloud conditions [21].

The MODIS LAI product is considered as having reached the second validation stage what means that it has been evaluated in several field studies over sufficient time periods, and all major biomes have been covered by analysis. Over all biomes, the LAI shows an accuracy of 0.66 (root mean squared error) according to the validation website of the MODIS Land Team [22]. Still, several problems persist even in the actual Collection 5 and the user is confronted with the problem of how to use the product data. This situation is reflected by the different approaches using MODIS LAI data and comparing it with other LAI data sources as well as the ongoing development of smoothing techniques and alternative algorithms [23–25]. Consequently, when combining MODIS LAI subsets with FLUXNET data the user has to make several decisions regarding the data post-processing: Which quality filter shall be applied? Should neighboring pixels be considered and if yes, how wide shall the data window be drawn in the 7x7 pixel subsets? Shall only Terra or Aqua data be used or shall they be combined? These questions have to be answered before methods are picked to fill missing data and smooth the time series as necessary.

Usually, MOD15A2, hence the more extensively validated Terra product, is downloaded by researchers, but [26] showed that there are no significant differences between the two sensors at the continental and tile scale and concluded that the combination of them helps to enlarge the number of high quality retrievals. However, on a pixel by pixel basis there occur large differences sometimes. The problem of choosing an appropriate LAI quality filter at FLUXNET sites has been tackled differently in MODIS LAI studies: All variations are used from selecting only those values signed as 'best' to no filtering: For example, [27] preferred data flagged as 'best', [28] and [29] recognized all 'good' data, [25] screened low quality data not marked at least as 'good' and those contaminated with clouds, [30] filtered out cloud contaminated pixels, and [31] averaged over all values. [26] advise to use back-up retrievals with care. Likewise, the question whether surrounding pixels should be taken into account and if yes how many pixels around the tower should be used has been answered differently by scientists: For example, only the central tower pixel is considered by [27]; in other studies, 3x3, 5x5 or 7x7 mean or median averaging windows are drawn around the tower pixel with the purpose of better representing the flux tower footprint and reducing geolocation and pixel-shift errors with the additional advantage of reducing the number of missing data points [31–33]. The latter problem of spatial and temporal discontinuity is an inherent characteristic of remote sensing data in the visible and near infrared due to the sensitivity of the radiance to cloud cover, snow and increased aerosol

Downloaded from SPIE Digital Library on 18 Jan 2011 to 128.219.49.8. Terms of Use: http://spiedl.org/terms

loading. Several studies have recently dealt with this problem and developed spatial-temporal smoothing, filtering and gap-filling techniques [18,25,34,35]. These approaches make, together with complex statistical and modeling techniques, again usage of quality flag and land class filtering as well as spatial averaging around a center pixel. However, the analysis of effects of these basic methods and their modification have been somewhat neglected in the literature.

In what follows, we analyze explicitly the effects of some fundamental post-processing methods on the magnitude, temporal variability and consistency of MODIS LAI values exemplarily at six FLUXNET sites of different vegetation classes from an end user perspective. Specifically, we illustrate the impact of several quality filters, assess the consequences of averaging over different window sizes around the tower pixel and compare Aqua and Terra subsets and consider the combination of them. Finally, the consequences on the output of a simple evapotranspiration model ('BUCKUP') resulting from different LAI input data sets are evaluated.

2 DATA

2.1 Study sites

Six FLUXNET test sites in North America are selected (Table 1): Duke Forest, North Carolina, USA, Howland, Maine, USA, Harvard Forest, Massachusetts, USA, Morgan Monroe State Forest (MMSF), Indiana, USA, Vaira Ranch, California, USA, and Lethbridge, Canada. These sites have been arbitrarily chosen between those featuring comprehensive multi-annual time-series with a good temporal coverage and being often used in the FLUXNET community (e.g. [36,37]).

Table 1. Characteristics of the study sites according to FLUXNET and LocClim, the FAO Local Climate Estimator [38]. Geographic location: latitude (lat), west longitude (long). h: elevation. Vegetation types (VT): evergreen needleleaf forest (ENF), deciduous broadleaf forest (DBF), grass (G). Koeppen-Geiger climate classes: C: temperate, D: continental, f: fully humid, s: summer dry, a: hot summer, b: warm summer. Temperature (T) and precipitation (P) are annual mean averages.

site	lat, long	h [m]	VT	climate	T [°]	P [mm]
Duke	35.98, 79.09	163	ENF	Cfa	14.4	1169
Howland	45.20, 68.74	60	ENF	Dfb	5.3	1070
Harvard	42.53, 72.17	340	DBF	Dfb	6.6	1071
MMSF	39.32, 86.41	275	DBF	Dfa	10.9	1032
Vaira	38.41, 120.95	129	G	Csa	15.9	544
Lethbridge	49.71, 112.94	960	G	Dfb	5.4	398

Duke Forest is an evergreen needleleaf forest plantation of about 25 years in a humid climate with mild winters and hot summers. Its overstorey almost solely consists of loblolly pine (Pinus taeda L.) with a mean height of about 20 m; 26 different hardwood species form the rich understorey [39]. In December of 2002 an ice storm damaged one third of the trees [40]. In the temperate continental Howland Forest, hardwoods such as red maple and paper birch (Betula papyrifera) occur among the dominating coniferous species as red spruce (Picea rubens), eastern hemlock (Tsuga canadensis), balsam fir (Abies balsamea), and white pine (Pinus strobus). The median stand-age of this boreal-northern hardwood transitional forest is about 100 years. The canopy height is estimated as 20 m [41]. Harvard Forest is mainly composed by deciduous broadleaf trees with a stand-age of about 80 years. The main species are red oak (Quercus rubra), red maple (Acer rubrum), black birch (Betula lenta), white pine (Pinus strobus), hemlock (Tsuga canadensis), white oak (Quercus alba), black oak (Quercus velutina), and hickory (Carya

Downloaded from SPIE Digital Library on 18 Jan 2011 to 128.219.49.8. Terms of Use: http://spiedl.org/terms

ovata) with a mean height of 23 m. The climate is characterized by cold winters and warm summers [42]. MMSF is also classified as deciduous broadleaf forest dominantly composed by sugar maple (Acer saccharum), tulip poplar (Liriodendron tulipifera), sassafras (Sassafras albidium), white oak (Quercus alba), black oak (Quercus nigra) with a mean age of almost 80 years. Cold winters and hot summers form a temperate continental climate [43].

The two selected grassland sites represent contrasting ecosystems: Vaira Ranch is located in the lower foothills of the Sierra Nevada Mountains on managed farmland. The C3 annual grasses grow in a Mediterranean climate with a distinct drought season in summer [44]. Lethbridge, however, east of the Canadian Rocky Mountains, is characterized by a humid climate with cold winters and warm summers. The short prairie consists of C3 and C4 species [45].

For all sites but Lethbridge, field measured LAI data were available via the website of AmeriFlux, the regional subdivision of FLUXNET. An overview on the time range with available measurements from 2002 to 2009, the number of measurements as well as remarks to the measurements can be found in Table 2.

Table 2. Available field measurements specified by the covered time range and the total number of sample dates within the whole time perid along with information on the measurements.

site	time range	number	measurement
Duke	2002-2005	8	Multiple techniques assimilated
Howland	2006	7	LAI-2000; 200 m transect every 10 m
MMSF	2002-2006	95	LAI-2000
Harvard	2005-2008	41	33 samples per date
Vaira Ranch	2002-2006	48	Li-Cor 3100, 4 samples per date

2.2 MODIS LAI data

As sensor on-board Terra and Aqua, two sun-synchronous and near-circular satellites, MODIS scans the earth surface every second day, above 40° latitude even every day with a swath width of 2330 km. The 36 spectral channels in the visible and infrared spectrum have a resolution of 0.4 to 14.4 m and a spatial resolution of 250 to 1000 m with the shorter wavelength having the greater resolution [46]. To retrieve the LAI products, namely MOD15A1 and MYD15A2, up to seven spectral bands are utilized to solve the inverse LAI problem with a radiative transfer model. The parameters for this model are stored in a look-up table specifically for eight biomes. If this main algorithm fails, a back-up algorithm is called which regresses the LAI on the basis of a empirical relationship between the LAI and NDVI (Normalized Difference Vegetation Index). The final product has a resolution of 1 km. The daily values are merged to 8-day composite products to reduce the impact of clouds and aerosols as disturbing factors, whereas the LAI of the day with the maximum FPAR value is selected for the respective 8-day period [47]. To create the MODIS Land Subsets, the LAI product is resampled in such a way that the center pixel of a 7x7 grid of 1-km pixels contains the FLUXNET tower. The subsets contain six values for every time step: a LAI as well as FPAR value, their standard deviations, a general and detailed quality criteria (QC). In this study, MOD15A2 and MYD15A2 are downloaded in ascii-format from the ORNL DAAC website [48]. The LAI and the general QC are extracted from both sensors.

The general QC provides four quality informations in 8 bits. One quality criterion is called 'MODLAND_Q' and allows a first check on the LAI quality. Since the algorithm path is the main factor influencing the LAI quality [26, 47], MODLAND_Q informs the user if the main algorithm was used, if the back-up algorithm had to fill in or if the value could not be retrieved at all. Another quality criterion indicates if the detector worked for up to 50 % of the channels or was mainly dead. The cloud state quality bit specifies if the pixel was clear, a significant cloud coverage or mixed clouds were present, or if the cloud status could not have been identified. Finally, additional details about the algorithm path are provided: A retrieval with the

Downloaded from SPIE Digital Library on 18 Jan 2011 to 128.219.49.8. Terms of Use: http://spiedl.org/terms

main algorithm without saturation is classified as 'best possible result', with saturation as 'good result'. Saturation means, the reflectances do not deliver precise information about the surface and the canopy radiation transfer model is insensitive to a set of possible canopy realizations, thus the probability for different LAI values is of the same magnitude. This situation occurs with increasing frequency for LAI values greater than 4 and affects almost every value greater than 5 since the reflectances at these high LAI values get more and more insensitive to LAI differences [47]. It is further stated in the detailed QC bits if the main algorithm failed and the back-up algorithm was used due to geometry problems or for other reasons than a bad geometry. A complete failure is the last possible outcome of the algorithm path analysis.

In this study, we consider following QC cases: unfiltered, cloudless, 'good' values, 'good' values without clouds, 'best' values, 'best' values without clouds, back-up retrieval and back-up retrieval without clouds. Terra began to provide MODIS data from the beginning of 2000, Aqua followed in April 2002. In this study, data from both sensors are recognized from the latter date when both MODIS products are available until September 2009.

2.3 MODIS land cover data

Additionally, the MODIS land cover product (MCD12Q1) retrieved with data from Terra and Aqua [49], is downloaded to further characterize the pixels around the tower and to filter pixels of strongly differing land classes. MCD12Q1 subsets are available for the years 2001 to 2005. They provide annual land class estimations around the tower with a spatial resolution of 250 m. Five land classifications are offered. For this study, the third land cover scheme, the so called 'MODIS-derived LAI/FPAR scheme' has been selected. This scheme distinguishes between 8 vegetation classes beside water, non-vegetated and urban classes: 1. Grasses and cereal crops, 2. shrubs, 3. broadleaf crops, 4. savanna, 5. evergreen broadleaf forests, 6. deciduous broadleaf forest, 7. evergreen needleleaf forest, 8. deciduous needleleaf forest. These eight classes are exactly those which are used in the LAI retrieval and have shown to be somewhat more reliable than the other classifications provided [50].

We assume there have been no substantial land use changes in the areas around the towers neither in the years 2001 to 2005 nor later on and generate a single land class map for all years by comparing the corresponding pixels of all five years. That land class is assigned to the pixel that at least occurs three times. After the temporal aggregation, the pixels are spatially aggregated: A mask with its resolution matching that of the LAI grid is generated, for what the four corresponding 250-m pixels of each 1-km pixel are examined. That land class which occurs at least at three of the four sub-pixels is assigned to the 1-km pixel. If no land class appears more than two times, this pixel is treated as unclassified and not considered in the further analysis. Additionally those pixels are excluded from the further study which have a completely different land cover and consequently not comparable LAI values in relation to the tower pixel. [25] have shown a land class selection to be superior for spatial aggregations. However, pixels with another but similar land classes are accepted for the further analysis. Our reason for this procedure is that the MODIS land cover product often seems to have difficulties to distinguish between similar vegetation classes, especially in inhomogeneous areas [7, 50]. However, misclassifications in relatively similar biomes have moderate consequences on the LAI retrieval [50]. For the coniferous, deciduous and mixed forest sites, all the forest classes 5 to 8 are considered as similar. The classes 1 to 4 serve as similar classes for the grassland sites. The classification problems are clearly evident in the downloaded subsets. For example, MOD12Q1 classification type 3 cannot detect the loblolly pine plantation within a hardwood forest, but identifies a broadleaf forest in the whole region around the tower. Additionally, many pixels are variantly classified as shrub, savanna and grass and evergreen and deciduous forest during the five years; the severe icestorm disturbances and the rich understorey certainly play a role in this context (see section 2.1). At the grassland sites, the grassland class alternates spatially and temporally with the savanna class and in some cases with the crop class. The center

Downloaded from SPIE Digital Library on 18 Jan 2011 to 128.219.49.8. Terms of Use: http://spiedl.org/terms

pixels at Vaira are even always classified as savanna. The other three study sites are relatively uniformly and stably classified. In what follows, only pixels around the tower are taken into account which have a similar land class as the known vegetation class of the FLUXNET site according to the method explained above.

3 ANALYSIS

3.1 Overview

In what follows, the frequency of occurrence of the various quality criteria and their effect upon the seasonal evolution and statistical characteristics of the analyzed LAI time series are investigated. The various data sets resulting from the application of quality criteria and the spatial aggregation from 3x3 to 7x7 pixels or mere usage of the tower pixel, respectively, are thereafter analyzed and presented. Subsequently, the Terra and Aqua data sets are directly compared and combined to a single time series. Finally, it is shown of which magnitude the differences of a simple evapotranspiration model are when using various MODIS LAI data sets as model input.

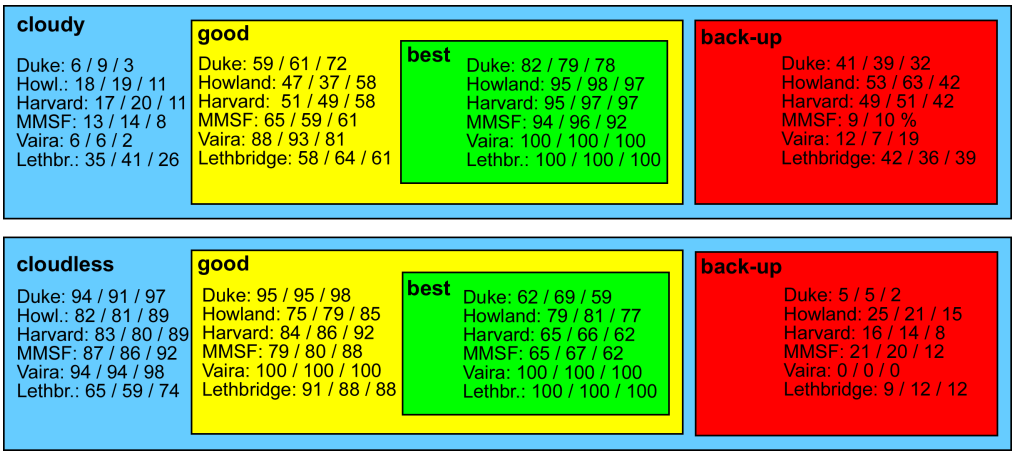

Fig. 1. Quality sets of MODIS LAI data used in this study. The number are percentages of the respective superordinate quality set for Terra, Aqua and the combined time series explained below (listed in this order in %). Cloudy and cloudless values are subsets of the whole quantity of LAI values. These sets characterized by the cloud state have subsets of back-up and 'good' quality sets. The sets of 'good' retrievals have a subset of 'best' values. The percentages refer to the directly superordinate set. This means i.e. for the LAI Terra data at Duke Forest, there are 6 % cloudy and 94 % cloudless retrievals. 95 % of the cloudless data are classified as 'good', only 5 % have been retrieved by the back-up algorithm; 62 % of the 'good' main algorithm retrievals achieve even a 'best' result.

3.2 Quality criteria

3.2.1 Occurrences of QC classes

To characterize the quality sets, the proportion of the various quality classes (unfiltered, 'good', 'best' and back-up) with and without clouds as percentage of all retrievals is quantified as a first step. Fig. 1 uncovers that significant more LAI values were retrieved under cloud-free than under cloudy conditions according to the QC bits (59 - 94 %). Aqua data tend to have a little more cloudy pixels than Terra data (up to 6%). Cloudy values have a higher percentage of back-up values. 68 to 100 % of all retrievals resulted in 'good' results via the main algorithm

Downloaded from SPIE Digital Library on 18 Jan 2011 to 128.219.49.8. Terms of Use: http://spiedl.org/terms

with the maximum number at Duke Forest and Vaira; at the latter site, the back-up algorithm has merely had to be triggered. Most 'good' values are associated with a clear sky (76 - 99 % of all 'good' values). Vice versa, the percentage of back-up values increases for cloudy pixels up to 53 % The 'best' retrievals make up 62 to 82 % of the 'good' set at the forest sites and almost all 'good' retrievals are 'best' at grassland sites, so barely no saturation occurred. Overall, about 50 to 64 % of all retrievals achieved a 'best' result, with the exception of Vaira, where almost all LAI values are rated as 'best'. Most 'good' values with clouds belong to the 'best' quality set with up to 98 % at forest sites. In contrast, the percentage of 'best' retrievals amount to 62 - 82 % of the cloud-free 'good' retrievals.

3.2.2 Seasonal evolution

As a second step to assess the impact of quality criteria on LAI time series, a visual inspection is carried out. For this purpose, Fig 2 plots the LAI-time series of all pixels for the various quality sets in following order of increasing filtering: all retrievals, 'good' retrievals, 'good' retrievals without clouds, 'best' retrievals, and 'best' retrievals without clouds. Earlier plotted values belonging to the 'lower', less stringent quality class are therefore covered by the dots of higher classes; values which are filtered out remain visible. What catches the eye first is a division of LAI values into two domains: 'best' values make up the LAI values from 0 to about 4 m^2m^{-2} and 'good' values without the 'best' are located above up to the maximum LAI. Even in summer, the LAI values are scattered almost throughout the whole range of LAI values. Unfiltered values which are not overlapped by the higher quality values, hence back-up values, appear in the whole LAI range, but tend to agglomerate in winter. Often they appear as a vertical sequence of dots, which can reach values that are lower or higher than the average at the considered time step. But beside the very low outliers in winter they form a time series that seems to be not different from higher quality data. In summer the back-up retrievals at high LAIs even tend to be not as noisy as the values flagged as 'good' and adopt values around the mean of 'good' values. Values from cloudy pixels, back-up retrievals and values in the 'best' set accumulate frequently in clusters in the lower LAI range.

The phenomenon of segmentation of the 'good' values in the saturation domain above 4 m^2m^{-2} and 'best' values at forest sites beneath it becomes even more apparent in the mean multi-year time series (Fig. 4): Whereas they are similar in winter, they diverge strongly in summer. The time series build from the 'best' values reach only about 60 % of the summer level of the time series resulting from the 'good' values. Since the set of 'good' comprises the 'best', the multi-year mean of the 'good' values without the 'best' retrievals in summer is even higher. This time series of the 'good' without the 'best' in summer is plotted in Fig. 3 and exhibits significant better seasonal dynamics than the unfiltered time series or the 'best' time series as shown in Fig. 2 in blue color. It is generated in the following way: As soon as the median of the 7x7 LAI values gets greater than 4 m^2m^{-2} in spring, all values are deleted which do not belong to the saturation domain ('best'). This approach is applied for the whole summer until the median of the LAI gets smaller than 4 m^2m^{-2} again. 4 m^2m^{-2} is chosen as a limit because the non-saturation frequency increases drastically according to the product's theoretical basis document [47]. And indeed, less than 2 %, in most cases even less than 1% of the 'best' values are greater than 4 m^2m^{-2}.

3.2.3 Statistical characteristics

In statistical terms, the single quality sets show differences, too. The means of the quality sets can be assigned to three groups of similar set means: Unfiltered values, retrievals without clouds, 'good' and 'good' values without clouds form a group of means, 'best' retrievals and those with clouds build another group with lower means, and back-up values, finally, present the third group with higher means with respect to the other groups. Since there are almost no 'good'

Downloaded from SPIE Digital Library on 18 Jan 2011 to 128.219.49.8. Terms of Use: http://spiedl.org/terms

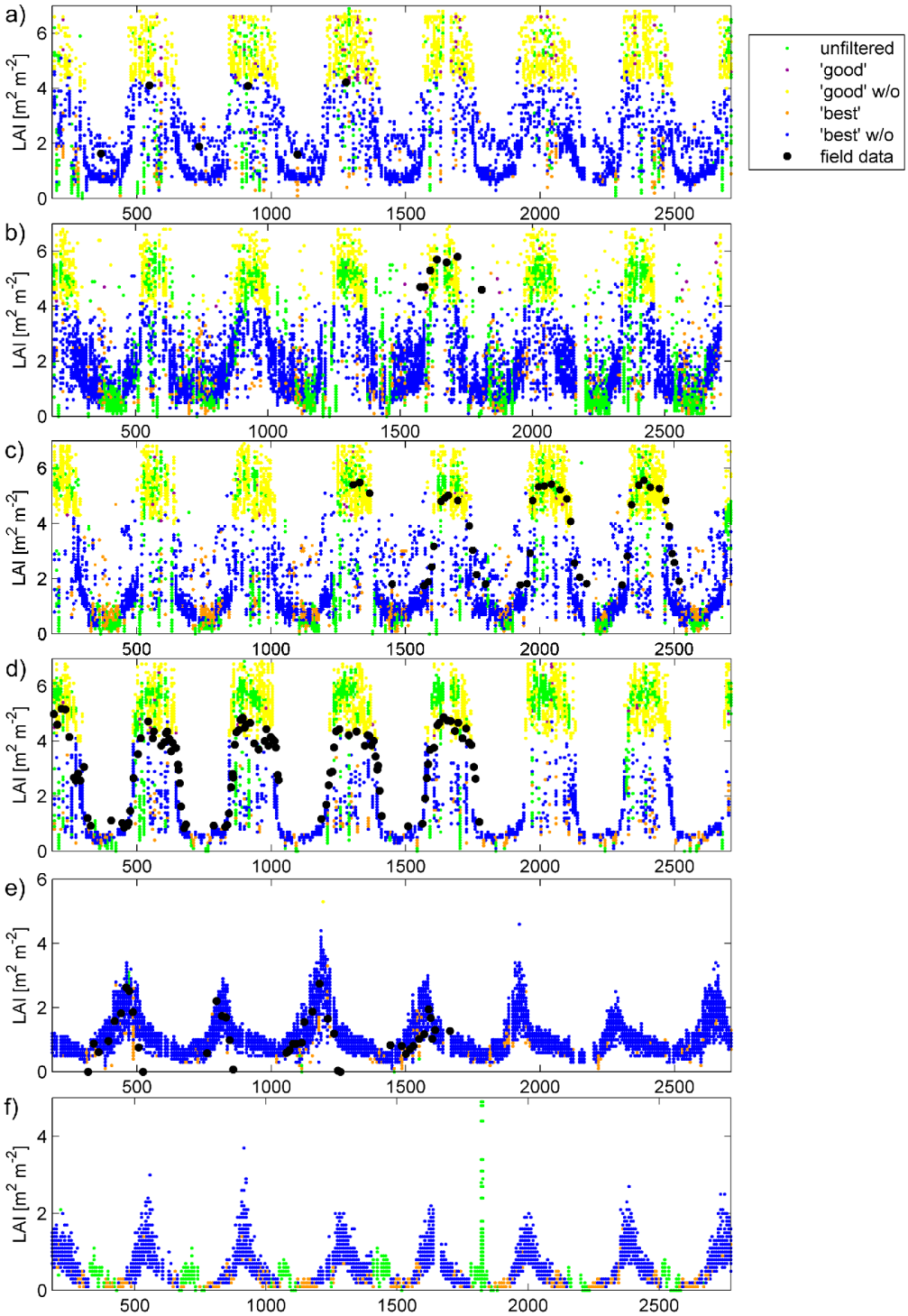

Fig. 2. LAI time series of the Aqua data sets at Duke (a), Howland (b), Harvard (c), MMSF (d), Vaira Ranch (e) and Lethbridge (f) showing the various quality criteria classes the LAI values belong to. These have been plotted in the order unfiltered, 'good','good' without clouds, 'best', 'best' without clouds. Dots plotted later cover previous plotted dots. LAI field data are plotted as a rough reference.

Downloaded from SPIE Digital Library on 18 Jan 2011 to 128.219.49.8. Terms of Use: http://spiedl.org/terms

values with saturation at grassland sites, hence 'good' values are also rated as 'best', only two groups can be identified: unfiltered and main algorithm values as well as back-up values. At the grasslands there is no tendency regarding the difference between the group means. Within all groups, retrievals from cloud-free pixels have a higher mean than their unfiltered counterparts, and a even higher mean than the cloud affected retrievals. The differences between the quality set means reach values in the range of the LAI magnitude of the unfiltered mean; at MMSF the difference between the back-up values and the 'best' amounts to nearly 4 LAI units. The medians of the quality sets are lower than the means, only the back-up medians are higher in a few cases. The medians have the same characteristics as the means, but show with up to 5 LAI units even higher differences between the quality sets. The analysis of the quality sets' variances draws a similar picture: lower variances of 'best' and cloudy values and higher for back-up retrievals compared to the unfiltered and 'good' retrievals. The average variance of time series without clouds is lower than that of the unfiltered time series. The differences between the temporal variance of each pixel of the 7x7 pixels when compared to each other are significant larger for time steps with clouds than without cloud coverage, so the temporal variances are much more unsteady.

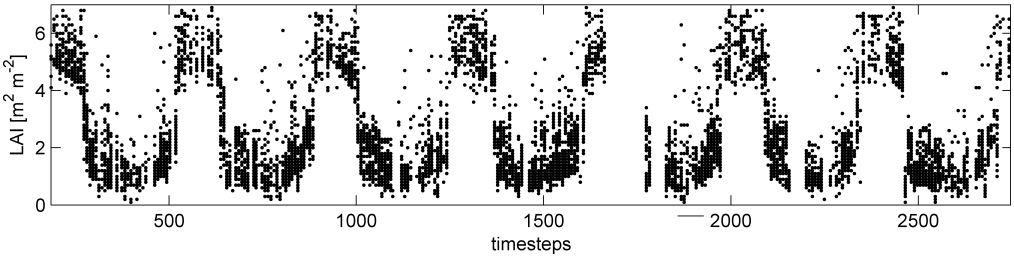

Fig. 3. The set of 'good' values without the 'best' values in summer. This time series of Terra at Howland is typical for the analyzed forest sites.

The LAI frequency distributions of the quality sets provide an explanation for the differing means and medians as Fig. 5 demonstrates: The unfiltered values show a frequency distribution with two peaks around 1 m^2m^{-2} as well as 5 m^2m^{-2}. The 'good' LAI values form a similar bimodal frequency distribution pattern with somewhat more distinct maxima at the most sites. Likewise, the frequency distribution of the back-up retrievals has two peaks, but these are shifted towards the upper and lower end of the LAI range. The 'best' values, however, exhibit an uni-modal distribution with a peak between 0 and 1 m^2m^{-2}. Most quality sets free of cloud contamination show a smaller occurrence of lower values and a higher occurrence of higher values; this shift to higher values is most distinctive for the back-up sets.

With the non-parametric Kolmogorov-Smirnov-test all quality sets are compared mutually with each other with respect to their frequency distributions. The results indicate that almost all quality sets at the forest sites can be assumed to have been drawn from different distributions with two exceptions: first, the different cloudy data sets of the main algorithm - which is simply a consequence of the fact that the most cloudy data from the 'good' set are classified as 'best' since they are in the lower LAI domain and hence not subject to saturation - and second, the 'good' values without clouds and the data set without non-saturation values in summer. At Duke Forest, the 'good' and the unfiltered set without clouds additionally comply with the null hypothesis that they are from the same distribution and the same is true for the 'best' sets with and without clouds. At the grassland sites, unfiltered quality sets and those of the main algorithm are found to be similar when they have the same cloud status; this similarity is not surprising since the classes share almost the same elements. The additionally executed Kruskal-Wallis hypothesis test, a one-way analysis of variance by ranks, draws a similar picture. In summary, the two applied hypothesis tests show the tendency of the 'best' sets being different from the

Downloaded from SPIE Digital Library on 18 Jan 2011 to 128.219.49.8. Terms of Use: http://spiedl.org/terms

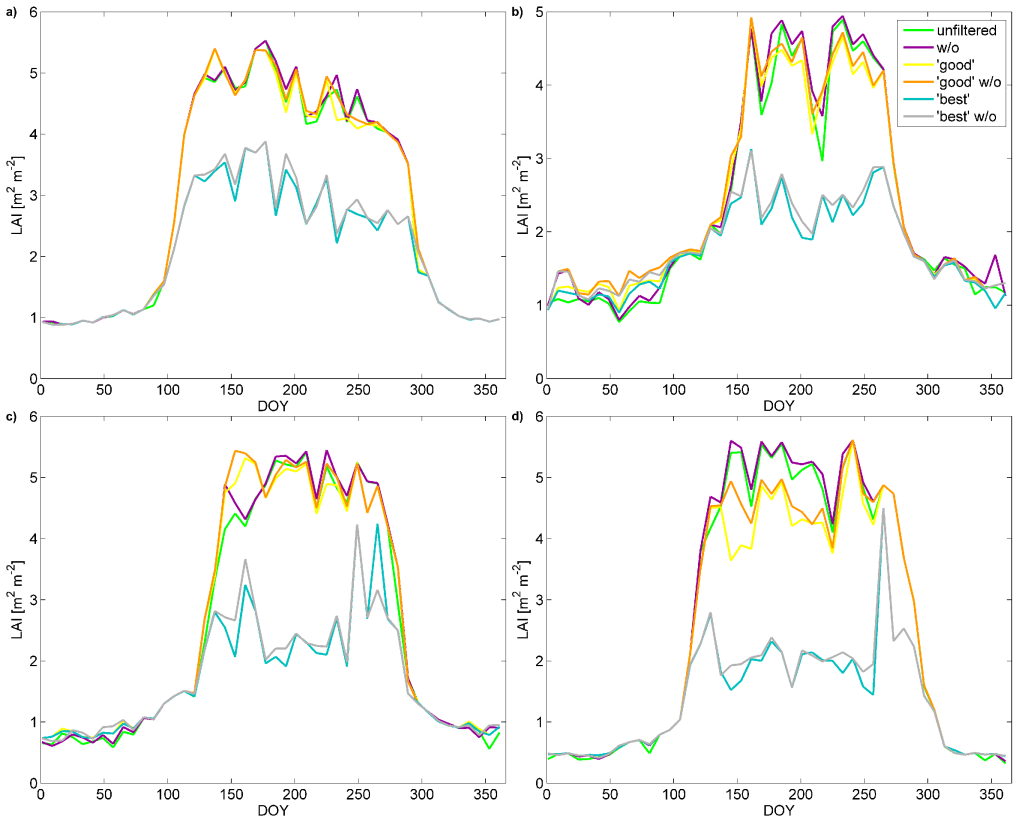

Fig. 4. Multi-year average of the various quality classes in the Terra data sets at Duke (a), Howland (b), Harvard (c), MMSF (d).

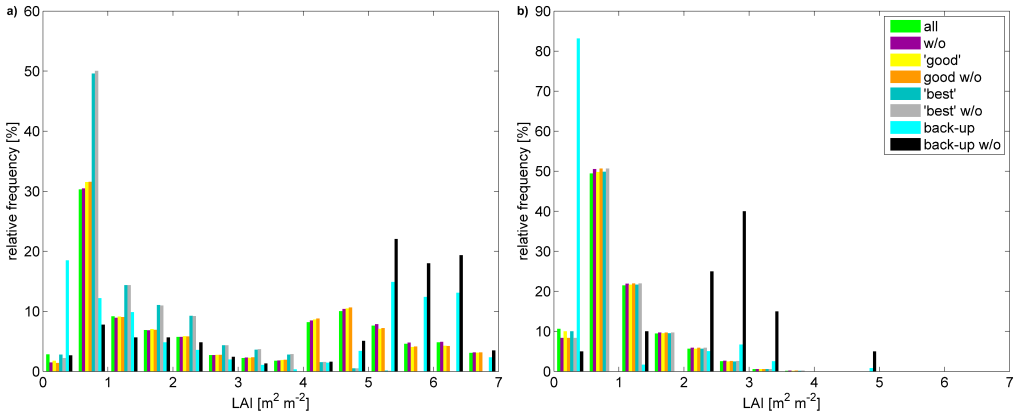

Fig. 5. Frequency distributions of the quality sets using the example of Terra data at Duke Forest and Vaira Ranch. Frequencies of the sets are relative to the number of all retrievals in the respective sets.

Downloaded from SPIE Digital Library on 18 Jan 2011 to 128.219.49.8. Terms of Use: http://spiedl.org/terms

other sets at the forest sites and the cloud state playing a significant role when comparing data sets.

3.2.4 Comparison with field data

A comparison with the available LAI field data is done as next step in comparing the quality sets. Since the LAI is not measured with the same methods at the test sites and the field measurement and MODIS scales are different the comparison is executed to show trends and not to validate the MODIS LAI data explicitly. The comparison shall serve as an additional piece of the puzzle of hints regarding the best usage of MODIS LAI data. A visual comparison in Fig. 2 reveals that the MODIS LAI follows quite good the seasonal LAI dynamics. In the critical summer season, the field measured LAI values from Harvard and Howland lie in the range spanned by the 'good' MODIS values, at Duke Forest and MMSF, however, the field data are located at the lower end of range of 'good' values. In winter, however, the MODIS LAI values rather underestimate the measured data at the needle leaf Duke Forest and tend to overestimate it at the broadleaf MMSF - a phenomenon which has been often reported before [51].

A quantitative comparison at the three sites with the longest field measured time series (Harvard, MMSF, Vaira) is carried out by applying the root mean squared error ($RMSE$), the bias (as difference between the means) as well as the Nash-Sutcliffe efficiency (EC). The EC is widely used in hydrology to evaluate modeled time series with measurements and is defined as the variance of residuals of predicted (P) and observed (O) values normalized by the variance of the observed values and subtracted from one:

$$EC = 1 - \frac{\sum_{i=1}^{n}(O_i - P_i)}{\sum_{i=1}^{n}(O_i - \bar{O})} \tag{1}$$

This quality criterion ranges from a value of one for a perfect fit to $-\infty$ whereas negative EC values indicate that the mean of the observed time series would have been superior to the predictor.

EC, $RMSE$ and bias show a comparable behavior of the unfiltered and 'good' values with respect to the field data at the forest sites (Fig. 6a). This is true for all spatial configurations from the exclusive use of the tower pixel to the exploitation of all 7x7 pixels with a similar land class available in the subset whereas it appears that the more pixels are taken into account the better is the match of field and remote sensing data. If the 'good' values subject to saturation are removed in summer comparison statistics improve a little bit. At MMSF and Duke, however, the 'good' values in the saturation domain are too high compared to the field data; the consequence is that the unfiltered LAI data compare best to the field data, since the too low 'best' values and the too high 'good' values in the saturation domain compensate each other. Taking only the 'best' values into account, however, the goodness of fit between field and MODIS LAI data deteriorates and results in a greater bias and $RMSE$ as well as a lower EC at the forest sites. The retrievals without clouds tend to be somewhat more concordant with the field measurements at all sites which is especially apparent at Vaira Ranch (Fig. 6b).

3.3 Spatial aggregation

Figure 6 discussed above has shown that the spatial aggregation by taking the mean of the considerd pixel window has an influence on the comparability with the field measurements: The more pixels around the tower are used, the better the field and MODIS data are comparable tendentially. Do the spatial aggregations also have an positive effect on the temporal consistency of the resulting time series? The temporal evolution during a typical year without extreme events as storms, drought or severe fires is supposed to be relatively smooth; MODIS LAI products, however, tend to show a higher temporal noise than expected in a phenologically sound sense [24, 29, 52].

Downloaded from SPIE Digital Library on 18 Jan 2011 to 128.219.49.8. Terms of Use: http://spiedl.org/terms

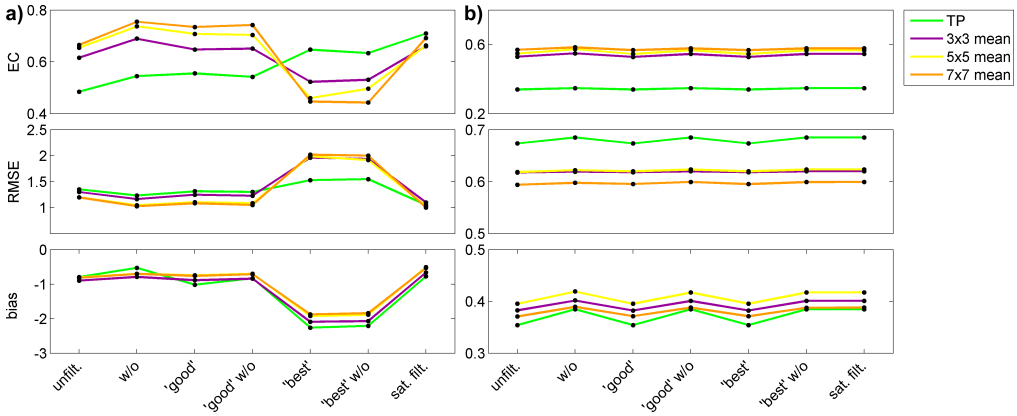

Fig. 6. Quality criteria for the comparison of field measured data with the MODIS LAI values for the various quality sets at Harvard (a) and Vaira Ranch (b). The tower pixel (TP) alone as well as the 3x3, 5x5, 7x7 pixels around the tower pixel are compared with the field measurements.

A comparison of the variances σ for the tower pixel and spatially aggregated time series shows indeed a decrease with an increasing pixel window size in the most cases, whereas at the same time, the means remain very similar for the aggregations, except for Howland Forest. An inspection of the Howland time series reveals lower values in winter for the more extensive aggregations, which is a consequence of a changing tree composition in favor of deciduous species; this assumption is supported by the MODIS land class map.

But to evaluate the smoothness of the time series, the magnitude of the up-and-downs at consecutive time steps is even more important, for what reason the smoothness measure δ is consulted. This method has already been used by [29] to compare the temporal consistency of MODIS and CYCLOPES LAI time series. δ calculates the difference for each time series element to the linearly interpolating line between its two adjacent neighbors:

$$\delta = (0.5 \cdot (LAI(t + \Delta t) + LAI(t - \Delta t))) - LAI(t) \tag{2}$$

A single drop of a time series element would for example lead to a high δ value at this time point, a sudden jump to a high negative value. Histograms of the relative frequencies of all occurring δ-values show indeed a change of the δ-distributions for the different spatial aggregations towards the low δ-bins for the aggregations compared to the tower pixels' δ-values: The greater the aggregation, the steeper is the decrease and the earlier the frequencies approach zero occurrences towards larger δ-bins (Fig. 7a).

As second method to measure the smoothness and noise of the LAI time series, frequency analysis is applied and realized with the Matlab® function 'spa', which calculates the frequency response and power spectrum of a signal using Fourier analysis. A smooth, periodic time series would result in a power spectrum with a sharp peak at low frequencies and low values at higher frequencies. A highly noisy time series would result in a large horizontal part in the power spectrum. The application of this method to the various aggregation show a faster drop of the power spectrum towards high frequencies, the larger the aggregation window around the tower pixel is. Figure 7b shows this behavior for Lethbridge. The aggregation not surprisingly tends to blur the difference between the quality sets (Fig. 7b); but still, the cloud filtered time series has a lower power spectrum at high frequencies and the main algorithm time series without clouds tends to show even more the characteristics of a slightly smoother time series. Using only the tower pixel makes it more important to understand and apply the quality flags because the difference between them gets larger (Fig. 7d). The frequency analysis also shows that the empirical back-up values are not necessarily more noisy than the main algorithm values.

Downloaded from SPIE Digital Library on 18 Jan 2011 to 128.219.49.8. Terms of Use: http://spiedl.org/terms

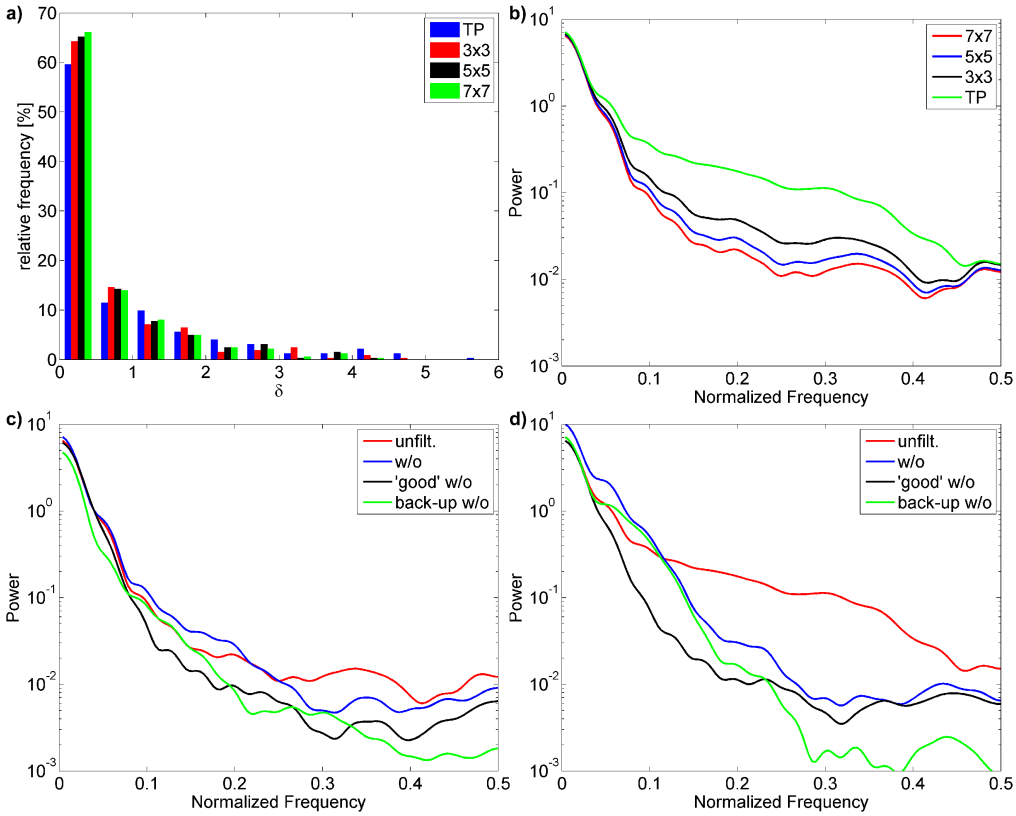

Fig. 7. Histogram of relative frequencies of δ for the spatial aggregations, namely for the time series of the tower pixel (TP) up to the averaged (median) 7x7 pixel window, exemplarily shown for the unfiltered MMSF Aqua data set (a). Power spectra for the aggregated Lethbridge data sets (b) and for the various quality classes for the 7x7 aggregation (c) as well as the tower pixel (d).

3.4 Comparison of Terra and Aqua data

3.4.1 LAI retrievals and quality classes

As a first step of the Terra-Aqua-analysis, we explore the questions of whether it is advantageous to combine MOD15A2 with MYD15A2. The number of overall retrievals would clearly profit from the combination of Terra and Aqua. In 6 to 7.4 % of all pixels and retrieval dates one value lacks in the Terra or Aqua data set but the other is available. In all but a few cases Aqua delivers 2 to 4 % more values than Terra which is mainly a consequence of a longer gap in the Terra time series in 2006. The proportions of the quality classes are similar in the two data sets. The greatest differences occur at Duke and Lethbridge with the Aqua data sets having 3 % or almost 7 %, respectively, less main algorithm retrievals without clouds than Terra. In at least 4 % of all retrieval dates, the pixel of one data set is cloudy, the other is not. The Canadian grassland Lethbridge experiences the greatest cloud coverage of about 40 %; the combination of the two sensors could reduce this amount to 26 %.

3.4.2 Statistical characteristics

But are the two data sets really comparable and hence combinable? Analyzing the statistical characteristics of the two data sets, it becomes evident that the overall means of Terra are slightly higher than those of the Aqua data sets (0.01 to 0.15 m^2m^{-2}), only at Duke, the bias

Downloaded from SPIE Digital Library on 18 Jan 2011 to 128.219.49.8. Terms of Use: http://spiedl.org/terms

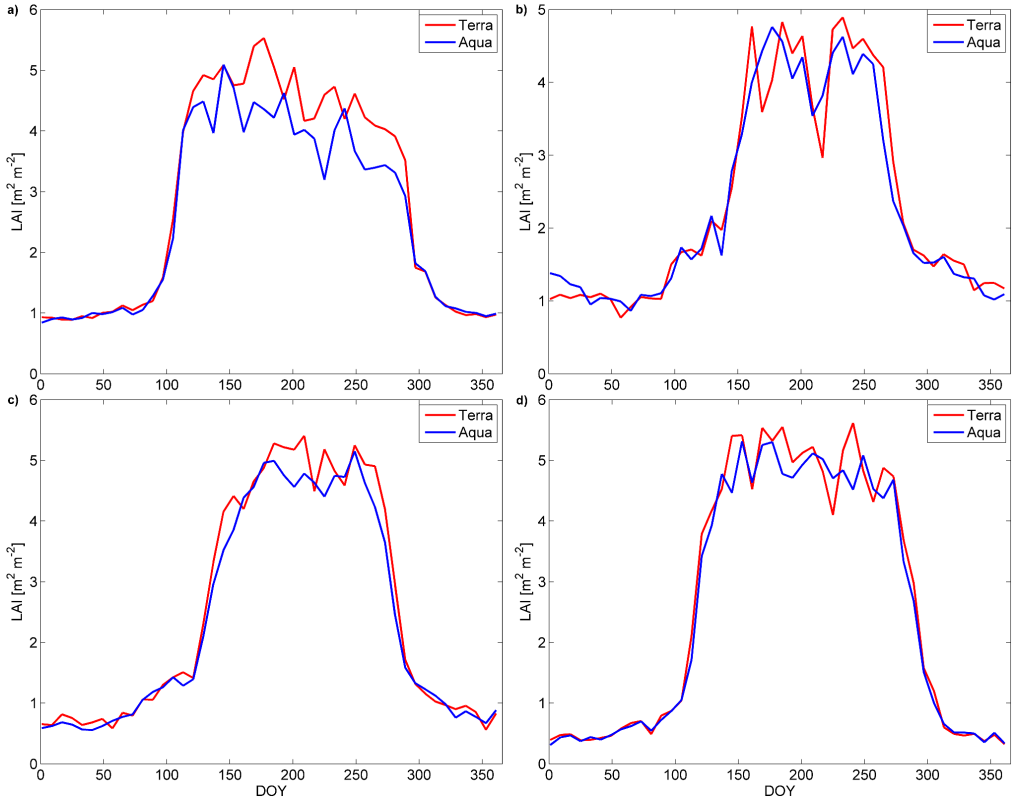

Fig. 8. Multi-year average LAI at a) Duke, b) Howland, c) Harvard, d) MMSF showing the long-term difference between the MODIS sensors onboard Terra and Aqua.

constitutes even nearly 0.3 m^2m^{-2}. The medians are equal in all cases, but again at Duke, the median differs even by 0.4 m^2m^{-2}. These differences get evident in the multi-year averaged LAI-dynamics (Fig. 8) as well as in the frequency distributions (Fig. 9): Average Terra values in summer are noticeably higher than the Aqua multi-year means, and the relative frequencies of Terra retrievals in the second half of the LAI range exceed the relative frequencies of Aqua retrievals. Vice versa, the Aqua data sets have relatively more LAI values in the lower LAI range. This is true for both forests and grasslands, even though the phenomenon is less distinctive at grassland sites.

The residuals of the two sets calculated as Terra minus Aqua values range up to 6 m^2m^{-2} in the forest data sets and up to 3 m^2m^{-2} at the grassland data sets. Their frequency distributions diverge from the normal distribution with a positive kurtosis and skewness rightwards, so the deviations do not seem to be random but systematic. The Kruskal-Wallis-test denies the null hypothesis that the two data sets are statistically similar and suggests that they are drawn from different populations. For higher quality data, the null hypothesis gets somewhat more probable. According to the RMSE, the differences range from 0.15 m^2m^{-2} (Lethbridge) to 1.35 m^2m^{-2} (Duke Forest).

Plotting the LAI values from the two data sets directly against each other (Fig. 10) and counting the occurrences in 0.1 m^2m^{-2} wide bins reveals different patterns at the forest and the grassland sites: In both biomes, the highest frequencies of data points occur around the 1:1 line of a perfect match between the two data sets. At grasslands, the data points in the sensor space form an elliptic-like shape with some few scattered points around it. At the four forest sites, however, the scatter pattern clusters in four parts: One part is similar to an ellipse around the 1:1 line at LAI-values up to 4 and contains the most values. After a gap with no or very

Downloaded from SPIE Digital Library on 18 Jan 2011 to 128.219.49.8. Terms of Use: http://spiedl.org/terms

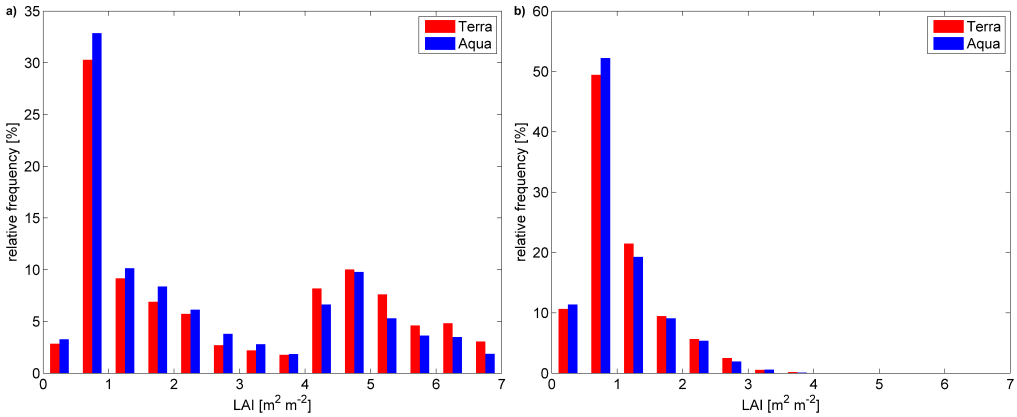

Fig. 9. Relative frequency of LAI values in bins of 0.5 LAI units as percentage of all retrievals in the subsets of a) Duke and b) Vaira. Relative frequency distributions at the other study sites are similar.

few values, this part is continued at along the 1:1 line at higher LAI-values by a second, wider cluster. Two additional clusters are located in the left upper and right lower quadrant of the scatter plot, namely at low Terra values and high Aqua values and vice versa. In summary, the data of Terra and Aqua are either very similar or very different, whereas the first possibility has a significantly higher probability, especially at low LAI values. Taking only values flagged as 'good' and without clouds into account, the clusters somewhat narrow, especially those two clusters indicating high differences get smaller and less dense.

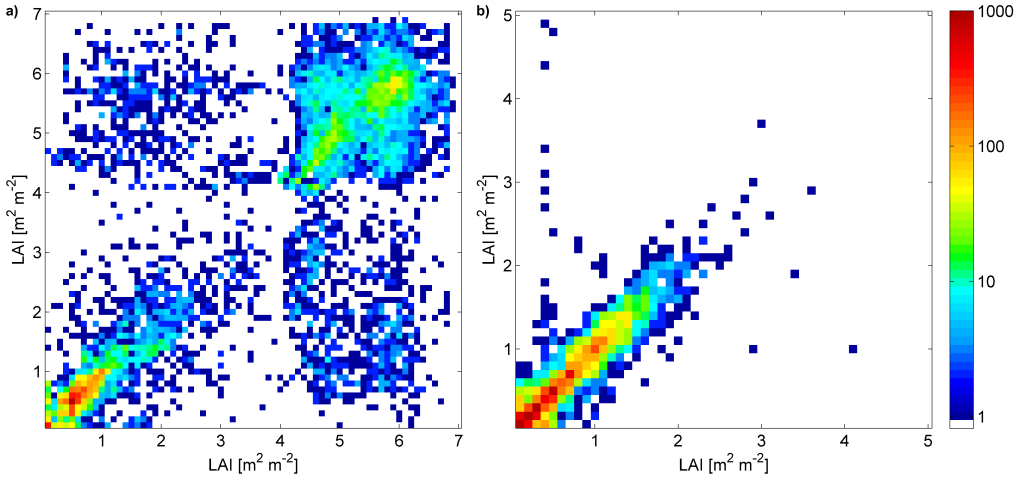

Fig. 10. Bivariate histograms of Terra (x-axes) and Aqua (y-axes) LAI values, exemplarily for a) MMSF and b) Lethbridge. White presents no occurrence, dark blue shows frequencies of 1, dark red frequencies of 1000 cases and more.

3.4.3 Combination

Despite the clues for systematic but compared to other criteria rather small differences between the Terra and Aqua data sets at these test sites, we apply a composition scheme. To generate the combined LAI values we follow the 'official' product combination approach [26] but enhance it with the lessons learned in this study regarding the influence of the cloud state. In doing so, we first compare the general quality criterion: If one was retrieved by the main algorithm

Downloaded from SPIE Digital Library on 18 Jan 2011 to 128.219.49.8. Terms of Use: http://spiedl.org/terms

and the other not, we prefer the 'good' value; if the algorithm path is equal we choose the cloud free retrieval; if the cloud state is also the same for both sensors, the LAI value with the higher corresponding FPAR value is taken since this value is assumed to be less atmospherically affected.

The advantage of the combined product is clearly the higher data availability as already mentioned above. Due to the preference of 'good' retrievals without clouds in the combination procedure, the number of these retrievals is enhanced by up to almost 20 % and the number of time steps at which at least 45 pixels 'good' retrievals without clouds are available rises by up to 40 % (Fig. 11). The temporal consistency as described by δ and frequency analysis is merely promoted by the combination procedure. The average temporal variance shows no decline, too. The spatial variance at each time step, however, tends to be moderated by the combination of the two sensors.

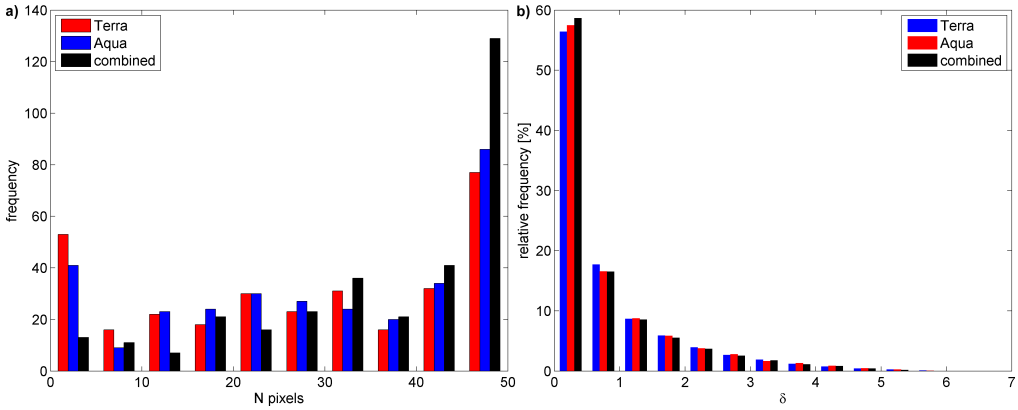

Fig. 11. The combined product shows an increased frequency of 'good' pixels without clouds for the combined product at every time step (a). The temporal consistency analyzed with δ , instead, shows only a small improvement for the combined time series (b). Plots shown for Howland.

3.5 Model sensitivity to LAI

The leaf surfaces represent the exchange medium between the plants and the atmosphere. The LAI as quantity for this exchange surface is consequently a critical variable for all biophysical models describing fluxes of energy, momentum and matter such as the exchange of carbon and water [53]. The index is of particular importance to modelers who want to upscale fluxes measured by eddy-covariance towers [54] or apply biomass models on a global basis or for agricultural purposes [55]. Since biosphere-atmosphere interactions are more and more implemented in global climate and hydrological models, the LAI is meanwhile also a key input variable for these model types [56, 57].

The Penman-Monteith equation is broadly applied in SVAT (soil-vegetation-atmosphere-transfer) models involving an estimation of the evapotranspiration [58] and is often executed depending on LAI [59, 60]. As a final part of the analysis we test the potential consequences of using various LAI time series based on different quality criteria on the calculation of latent heat fluxes. To do so, the simple bucket type SVAT-scheme 'BUCKUP' [61, 62] based on the Penman-Monteith equation is chosen and executed for the 2004 data of MMSF in a slightly modified mode:

$$\lambda E = \frac{\Delta R_N + (\rho c_p \delta q)/r_a}{\Delta + \gamma\,[1 + (r_s/r_a)]} \tag{3}$$

Downloaded from SPIE Digital Library on 18 Jan 2011 to 128.219.49.8. Terms of Use: http://spiedl.org/terms

with $\lambda E \left[W\ m^{-2}\right]$ being the latent heat flux, $\Delta \left[kg\ kg^{-1}\ K^{-1}\right]$ the rate of change of saturated specific humidity with temperature, $R_n \left[W\ m^{-2}\right]$ the net radiation, $\rho \left[kg\ m^{-3}\right]$ the dry air density, $c_p \left[J\ kg^{-1}\ K^{-1}\right]$ the specific heat of air, $\delta q \left[kg\ kg^{-1}\right]$, $\gamma \left[kg\ kg^{-1}\ K^{-1}\right]$ the psychrometric constant, and finally the surface and aerodynamic resistances r_s and r_a in $\left[s\ m^{-1}\right]$. While root zone water storage mainly controls water availability , the canopy and upper soil interception store, the root zone store as well as a variable ground water table act as evapotranspiration sources. Rainfall fills the interception store up to its limit. The interception overflow is assigned to the root zone store whose excess water is transferred to the groundwater table with a soil dependent time delay. The surface resistance r_s is updated every time step according to the actual water availability of the three stores. In this study, BUCKUP is extended by considering LAI seasonality: r_s is assumed to depend inversely proportional to the LAI [53]. Furthermore, the LAI is supposed to alter r_a by means of the displacement height, D, as well as the roughness length, RL according to the empirical relations [63] specified in the Appendix A. The model is run with hourly time steps using temperature, precipitation and humidity as meteorological boundary conditions. As LAI time series input we use the data from Terra, Aqua as well as the combined data set for the quality classes used in this study. For the combined product, the various spatial aggregations from the mere use of the tower pixel up to the 7x7 pixels are applied.

Since the model needs temporally continuous LAI data, we have to use an interpolation method. At the same time, we want to smooth the time series, since even the time series from taking the mean of all 7x7 pixels appears not to be physiologically sound. Interpolating and smoothing for model purposes has been proposed by other authors, too [18, 25, 33–35], which have used spatial averaging, upper LAI envelope smoothing techniques, adaptive Savitzky-Golay filtering, asymmetric and double logistic Gaussian filtering or an ecosystem curve fitting method based on the MODIS vegetation continuous fields product. In this exercise we want to give the noisy MODIS LAI data as much weight as possible but at the same time fulfill the contradictory demand of reducing the noise and the influence of outliers. Therefore, we choose a combined temporal-spatial interpolation scheme with a cubic smoothing spline method (see Appendix B). Figure 12a shows the results of this interpolation and smoothing procedure to daily LAI values for the combined Terra and Aqua data and the various quality data sets.

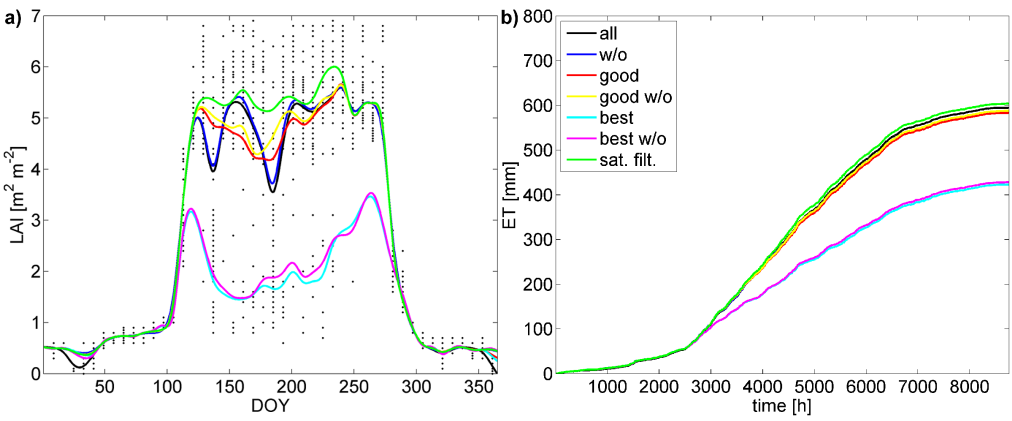

Fig. 12. (a) MODIS LAI (dots) and interpolated/smoothed LAI time series (lines) of different quality sets at MMSF, 2004. ”w/o” means data without clouds, ”sat. filt.” denotes the data set of ’good’ values without clouds and without LAI values in summer outside the saturation domain as described above. (b) Cumulative evapotranspiration for the different LAI input data.

The results of the sensitivity analysis illustrated in Figure 12b) show that the influence of the sensor choice as well as the quality criteria on the model output is rather small which is not

Downloaded from SPIE Digital Library on 18 Jan 2011 to 128.219.49.8. Terms of Use: http://spiedl.org/terms

surprising since the smoothing blurs the differences between the data sets. However there is one drastic exception: The 'best' values produce over 30 % lower cumulative amounts of evapotranspiration compared to the measurements and over 25 % compared to the results without using 'best' LAI values in summer. This is the case because the model evapotranspiration does not reach the high evapotranspiration values at daytimes in summer due to the much lower LAI values. This behavior will have a large impact on the subsequent prediction of individual components of the water cycle such as groundwater recharge or run off. Also, patterns of surface soil moisture availability will be largely biased and estimates of e.g. net primary production or bio-geochemical processes might be unreliably affected. Fact is, that the LAI time series at temperate forest sites get more unreliable in the sense of physiologically plausible temporal behavior when using the strictest quality filtering 'best' and this is true even when exploiting the data sets of both sensors.

4 DISCUSSION AND CONCLUSIONS

MODIS data from Terra and Aqua sensors in combination with ecosystem exchange data collected from FLUXNET have become central to the development, calibration and evaluation of soil-vegetation atmosphere transfer models (SVAT) and their regionalization. MODIS land product subsets provided for long term field measurement sites as from FLUXNET simplify the assimilation of field and remote sensing measurements for practical usage. Despite the frequent application of MODIS LAI subset data in ecosystem models, there is no consensus on their post-processing usage and the employment of the provided QC information. In this study we have analyzed the consequence of several post-processing user choices for six MODIS LAI subsets at FLUXNET sites (four forests, two grasslands) on the statistical characteristics and temporal behavior of the resulting LAI time series. The application of quality assessments as well as differing spatial aggregations from the only use of the tower pixel to the aggregation of all 7x7 pixels have been studied. The resulting various time series have been compared to ground-measured LAI values. The data from both sensors have been compared and their combination has been considered. Finally, the influence of differing post-processing choices on a simple SVAT model has been assessed.

The analysis of the quality criteria showed that most Terra and Aqua LAI values have been retrieved with the main algorithm and without cloud coverage what is an improvement compared to earlier MODIS LAI data collections. This fact has already been shown by [26] for a provisional collection 5 analysis. The spatial variation within the 7x7 pixels is high and the pixels' time series are often unstable and vary through the whole LAI range from near 0 to over 6 m^2m^{-2}. Cloud filtered time series and main algorithm time series tend to be smoother than their unfiltered counterparts. Most interesting is however the difference between 'best' and 'good' values from the main algorithm: 'best' values without saturation are significantly lower than main algorithm retrievals in the saturation domain and - by definition - seldom reach for forests realistic summer LAI values greater than 4 m^2m^{-2}. [64] mentions this phenomenon for forest sites, too. After the deletion of 'best' values in summer, the LAI time series shows - although with a considerable range of dispersion - a physiologically sounder temporal evolution. 'best' values in summer compare not as good to field data as the other quality sets. The unfiltered data sets perform well due to compensation effects of too high saturation domain values and too low 'best' LAI values. This is especially true for Duke Forest where the MODIS time series exceeds the ground-measured LAI values by over 2 m^2m^{-2}; one reason for this observation is certainly the land cover classification problem (see section 2.3) as well as general algorithm problems for coniferous forests [27, 65].

Are 'best' values in summer at forest sites just an artifact of cloudy conditions which have not been detected by the algorithm or the consequence of an erratic atmospheric correction? The fact that the most main algorithm retrievals with clouds are also 'best' retrievals supports this assumption as well as the fact that cloudy pixels have the tendency to have lower LAI

Downloaded from SPIE Digital Library on 18 Jan 2011 to 128.219.49.8. Terms of Use: http://spiedl.org/terms

values [26, 27]. Consequently, the end user has to take care when filtering according to the supposedly most stringent QC, 'best'; the semantic meaning of this adjective can be misleading when dealing with pixels covered by forests. Nonetheless, the study showed the benefit of using the provided QC meta data.

The question of spatially aggregating pixel around the tower or not has certainly to be answered from an site specific perspective and depends on the land cover classes involved and their distribution around the tower. If the emphasis is put on reducing the noise and increasing the data basis for interpolation and smoothing algorithms to build a more robust seasonal variation of LAI, as many pixels as the land cover distribution around the tower allows should be selected. The analysis showed that the smoothness, hence the temporal consistency, of the time series is enhanced using more pixels. This is consistent with the findings of [25]: In their data denial exercise to test several interpolation schemes, they used even 9x9 pixels and found it to be as good or even superior compared to 5x5 aggregations with having a higher data coverage at the same time.

The issue of spatial aggregation is tightly connected to three other post-processing options for MODIS Land Product Subsets, namely the selection of pixels according to specific land classes or other criteria as well as the interpolation and smoothing of the time series. The effects of filtering pixels around the tower on the basis of the MODIS land classification on the resulting LAI time series have not been analyzed in this study; this aspect needs further attention in future work. It will also be worthwhile considering to select pixels with respect to the footprint of the flux tower which depends mainly on the wind speed and direction. How to interpolate and smooth the LAI time series can certainly be discussed further: as [25] comments, there is no single interpolation scheme that can serve all purposes and conditions. Further analysis could analyze the benefits of using a weighting factor according to the LAI standard deviation delivered in the MODIS product.

Comparing the Terra and Aqua LAI retrievals at the six test sites, a small bias between the data sets was observed and pixel by pixel comparisons reveal large differences at a small proportion of the data. These observed large discrepancies for a limited number of data values can certainly be attributed to atmospheric conditions which are challenging for the algorithm. The cause for the systematic difference is not as obvious. [26] also observed a bias in Terra and Aqua reflectances and NDVI values at Harvard Forest. They excluded solar zenith angle and cloud influences and ascribed the discrepancies to erroneous atmospheric corrections, too. It is also known that Aqua suffers of band-to-band misregistrations of its MODIS sensor in the Visible and Infrared [66]; it is unclear, however, how this problem affects the LAI retrievals. In spite of the observed bias, [26] suggested the use of both products. Furthermore, we argue that the difference between the means of the Terra and Aqua product is small compared to the overall noise of the time series. Consequently, we have taken advantage of both LAI products and combined them as described in section 3.4.3 to further increase the reliability of the LAI time series. The combination of the two data sources increases the percentage of 'good' retrievals without cloud coverage by up to 17%. This is consistent with [26] who found a high quality retrieval increase of 10-20% for woody vegetation. The number of time steps with at least 45 'good' pixels without clouds increases by an amount of up to 40%. However, the temporal smoothness of the LAI time series is not improved (see section 3.4.3).

Also, we have analyzed the sensitivity of a simple SVAT model to the differently post-processed LAI input data. Predicted rates of evapotranspiration confirmed the previous findings: The use of 'best' data introduces a large bias of up to 40 % with possibly tremendous consequences on the subsequent prediction of individual components of the water balance. However, these consequences need further investigation and have to be extended to other related research areas.

Merging all analysis results, we can draw the conclusion that it is advantageous to combine Terra and Aqua to enhance the data coverage and maximize the number of cloud-free main-

Downloaded from SPIE Digital Library on 18 Jan 2011 to 128.219.49.8. Terms of Use: http://spiedl.org/terms

algorithm retrievals and follow one of two major strategies: to apply no QC filtering and take all pixels from the subset into account to achieve error nullification, or, alternatively, to make QC adjustments such as deleting back-up retrievals and those from cloudy pixels as well as 'best' retrievals belonging to the non-saturation domain when the retrieval can be expected to belong the saturation domain.

In this study we have discussed the usage of MODIS LAI data from an end-user point of view. Even though the product is considered as validated it is important to analyze usage options available to the modeler and quantify their effects on the resulting LAI time series. And even if product problems and possible pitfalls for the end user have been revealed by this and other studies, this extensive MODIS LAI database belongs without doubt to the most valuable information sources on vegetation dynamics the model community has.

APPENDIX A: THE EXTENDED BUCKUP MODEL

The original BUCKUP model as described by [62] is extended in this study by making the surface resistance r_s and the aerodynamic resistance r_a dependent on the LAI value at each time step. In doing so, r_s is defined to be reciprocally proportional to the LAI. r_a is indirectly modified by the the displacement height D and the roughness length RL according to following empirical equations [63]:

$$X = 0.2 * LAI \tag{4}$$

$$D = H * (log(1 + \sqrt[6]{X}) + 0.03 * log(1 + X^6)) \tag{5}$$

$$RL = H_U + 0.3 * H * \sqrt{X}\ forX < 0.2) \tag{6}$$

$$RL = 0.3 * H * (1 - D/H) forX >= 0.2) \tag{7}$$

where H is the vegetation height and H_U the understorey height. D and RL are then used to calculate r_a empirically. Details can be found in [67].

APPENDIX B: THE SMOOTHING SPLINE METHOD

To interpolate and smooth the time series of all 7x7 LAI values at each time step, a smoothing spline method as implemented in Matlab® as "csaps" is employed. The smoothing spline f minimizes

$$p \sum_{w(j)}^{n} |y(:,j) - f(x(j))|^2 + (1-p) \int \lambda(t) \left| D^2 f(t) \right|^2 \tag{8}$$

where x represents in this case the time vector and y the LAI data, j runs from 1 to the maximum number of entries of the temporal data vector, n. D^2 denotes the second derivate. Further, λ is a weight function and w a weight vector which is set to 1 in this study. p represents a smoothing parameter; it is chosen by the algorithm depending on the LAI values at each time step. Several data points at the same time steps are recognized as the average. csaps is an implementation of the FORTRAN routine 'SMOOTH' [68].

Acknowledgments

This work was funded by the Deutsche Forschungsgemeinschaft (DFG). Data from the Fluxnet sites were provided by the AmeriFlux web data archive supported by the U.S. Department of Energy (DOE), Department of Commerce, Department of Agriculture, National Aeronautics and Space Administration (NASA) and the National Science Foundation. MODIS LAI subsets were downloaded from the NASA-sponsored Oak Ridge National Laboratory Distributed Active Archive Center (ORNL DAAC). We thank Heather R. McCarthy for generating the LAI data at Duke Forest with support by the Office of Science (BER) U.S. Department of Energy, and J. William Munger for making the LAI measurements at Harvard Forest available. We thank

Downloaded from SPIE Digital Library on 18 Jan 2011 to 128.219.49.8. Terms of Use: http://spiedl.org/terms

David Hollinger and Andrew Richardson for providing the LAI data at Howland Forest, as well as Dennis Baldocchi for offering the LAI data from the Vaira Ranch site. Finally, we thank Danilo Dragoni funded by the U.S. Department of Energy Terrestrial Carbon Processes program (DOE TCP) for his helpful comments on the manuscript and for supporting the analysis by providing data from the Morgan Monroe State Forest study site.

References

[1] D. D. Baldocchi, B. B. Hicks, and T. P. Meyers, "Measuring biosphere-atmosphere exchanges of biologically related gases with micrometeorological methods," *Ecology* **69**(5), 1331–1340 (1988). [doi:10.2307/1941631].

[2] R. Stoeckli, D. M. Lawrence, G. Y. Niu, K. W. Oleson, P. E. Thornton, Z. L. Yang, G. B. Bonan, A. S. Denning, and S. W. Running, "Use of FLUXNET in the community land model development," *J. Geophys. Res. Biogeosci.* **113**(G1) (2008). [doi:10.1029/2007JG000562].

[3] M. Williams, A. D. Richardson, M. Reichstein, P. C. Stoy, P. Peylin, H. Verbeeck, N. Carvalhais, M. Jung, D. Y. Hollinger, J. Kattge, R. Leuning, Y. Luo, E. Tomelleri, C. M. Trudinger, and Y. P. Wang, "Improving land surface models with Fluxnet data," *Biogeosciences* **6**(7), 1341–1359 (2009). [doi:10.5194/bg-6-1341-2009].

[4] S. W. Running, D. D. Baldocchi, D. P. Turner, S. T. Gower, P. S. Bakwin, and K. A. Hibbard, "A Global Terrestrial Monitoring Network Integrating Tower Fluxes, Flask Sampling, Ecosystem Modeling and EOS Satellite Data," *Remote Sens. Environ.* **70**(1), 108–127 (1999). [doi:10.1016/S0034-4257(99)00061-9].

[5] M. E. Schaepman, S. L. Ustin, A. J. Plaza, T. H. Painter, J. Verrelst, and S. L. Liang, "Earth system science related imaging spectroscopy - An assessment," *Remote Sens. Environ.* **113**, S123–S137 (2009). [doi:10.1016/j.rse.2009.03.001].

[6] T. B. Wilson and T. P. Meyers, "Determining vegetation indices from solar and photosynthetically active radiation fluxes," *Agric. For. Meteorol.* **144**(3-4), 160–179 (2007). [doi:10.1016/j.agrformet.2007.04.001].

[7] W. B. Cohen, T. K. Maiersperger, Z. Q. Yang, S. T. Gower, D. P. Turner, W. D. Ritts, M. Berterretche, and S. W. Running, "Comparisons of land cover and LAI estimates derived from ETM+ and MODIS for four sites in North America: a quality assessment of 2000/2001 provisional MODIS products," *Remote Sens. Environ.* **88**(3), 233–255 (2003). [doi:10.1016/j.rse.2003.06.006].

[8] F. Baret, J. T. Morissette, R. A. Fernandes, J. L. Champeaux, R. B. Myneni, J. Chen, S. Plummer, M. Weiss, C. Bacour, S. Garrigues, and J. E. Nickeson, "Evaluation of the representativeness of networks of sites for the global validation and intercomparison of land biophysical products: Proposition of the CEOS-BELMANIP," *IEEE Trans. Geosci. Remote Sens.* **44**(7), 1794–1803 (2006). [doi:10.1.1.70.7416].

[9] C. O. Justice, E. Vermote, J. R. G. Townshend, R. Defries, D. P. Roy, D. K. Hall, V. V. Salomonson, J. L. Privette, G. Riggs, A. Strahler, W. Lucht, R. B. Myneni, Y. Knyazikhin, S. W. Running, R. R. Nemani, Z. M. Wan, A. R. Huete, W. van Leeuwen, R. E. Wolfe, L. Giglio, J. P. Muller, P. Lewis, and M. J. Barnsley, "The Moderate Resolution Imaging Spectroradiometer (MODIS): Land remote sensing for global change research," *IEEE Trans. Geosci. Remote Sens.* **36**(4), 1228–1249 (1998). [doi:10.1109/36.701075].

[10] A. Huete, K. Didan, T. Miura, E. Rodriguez, X. Gao, L. Ferreira, *et al.*, "Overview of the radiometric and biophysical performance of the MODIS vegetation indices," *Remote Sens. Environ.* **83**(1), 195–213 (2002). [doi:10.1016/S0034-4257(02)00096-2].

[11] J. Roehrig and R. Laudien, "Evaluation of agricultural land resources by implementing a computer-based spatial decision support system for national deciders in Benin, West Africa," *J. Appl. Remote Sens.* **3**(1), 033502 (2009). [doi:10.1117/1.3079033].

Downloaded from SPIE Digital Library on 18 Jan 2011 to 128.219.49.8. Terms of Use: http://spiedl.org/terms

[12] R. B. Myneni, S. Hoffman, Y. Knyazikhin, J. L. Privette, J. Glassy, Y. Tian, Y. Wang, X. Song, Y. Zhang, G. R. Smith, A. Lotsch, M. Friedl, J. T. Morisette, P. Votava, R. R. Nemani, and S. W. Running, "Global products of vegetation leaf area and fraction absorbed PAR from year one of MODIS data," *Remote Sens. Environ.* **83**(1-2), 214–231 (2002). [doi:10.1016/S0034-4257(02)00074-3].

[13] D. J. Watson, "Comparative physiological studies on the growth of field crops. 1. variation in net assimilation rate and leaf area between species and varieties, and within and between years," *Annals of Botany* **11**(41), 41–76 (1947).

[14] N. J. J. Breda, "Ground-based measurements of leaf area index: a review of methods, instruments and current controversies," *J. Exp. Bot.* **54**(392), 2403–2417 (2003). [doi:10.1093/jxb/erg263].

[15] S. W. Running, R. R. Nemani, D. L. Peterson, L. E. Band, D. F. Potts, L. L. Pierce, and M. A. Spanner, "Mapping regional forest evapotranspiration and photosynthesis by coupling satellite data with ecosystem simulation," *Ecology* **70**(4), 1090–1101 (1989). [doi:10.2307/1941378].

[16] F. Ewert, "Modelling plant responses to elevated CO_2: How important is leaf area index?," *Annals of Botany* **93**(6), 619 (2004). [doi:10.1093/aob/mch101].

[17] A. Lindroth, F. Lagergren, M. Aurela, B. Bjarnadottir, T. Christensen, E. Dellwik, A. Grelle, A. Ibrom, T. Johansson, H. Lankreijer, *et al.*, "Leaf area index is the principal scaling parameter for both gross photosynthesis and ecosystem respiration of Northern deciduous and coniferous forests," *Tellus Ser. B* **60**(2), 129–142 (2008). [doi:10.1111/j.1600-0889.2007.00330.x].

[18] Y. X. Gu, S. Belair, J. F. Mahfouf, and G. Deblonde, "Optimal interpolation analysis of leaf area index using MODIS data," *Remote Sens. Environ.* **104**(3), 283–296 (2006). [doi:10.1016/j.rse.2006.04.021].

[19] S. Wagner, H. Kunstmann, A. Bárdossy, C. Conrad, and R. Colditz, "Water balance estimation of a poorly gauged catchment in west africa using dynamically downscaled meteorological fields and remote sensing information," *Phys. Chem. Earth.* **34**(4-5), 225–235 (2009). [doi:10.1016/j.pce.2008.04.002].

[20] R. B. Myneni, R. R. Nemani, and S. W. Running, "Estimation of global leaf area index and absorbed PAR using radiative transfer models," *IEEE Trans. Geosci. Remote Sens.* **35**(6), 1380–1393 (1997). [doi:10.1109/36.649788].

[21] R. Myneni, Y. Knyazikhin, J. Glassy, P. Votava, and N. Shabanov, "User's Guide: FPAR, LAI (ESDT: MOD15A2) 8-day Composite NASA MODIS Land Algorithm," (2003).

[22] R. Myneni, "MODIS land team validation status for: LAI/FPAR (MOD15)." (Nov. 2009) http://landval.gsfc nasa.gov/ProductStatus.php?ProductID=MOD15.

[23] R. Houborg, H. Soegaard, and E. Boegh, "Combining vegetation index and model inversion methods for the extraction of key vegetation biophysical parameters using Terra and Aqua MODIS reflectance data," *Remote Sens. Environ.* **106**(1), 39–58 (2007). [doi:10.1016/j.rse.2006.07.016].

[24] J. Pisek and J. M. Chen, "Comparison and validation of MODIS and VEGETATION global LAI products over four BigFoot sites in North America," *Remote Sens. Environ.* **109**(1), 81–94 (2007). [doi:10.1016/j rse.2006.12.004].

[25] J. S. Borak and M. F. Jasinski, "Effective interpolation of incomplete satellite-derived leaf-area index time series for the continental United States," *Agric. For. Meteorol.* **149**(2), 320–332 (2009). [doi:10.1016/j.agrformet.2008.08.017].

[26] W. Yang, N. V. Shabanov, D. Huang, W. Wang, R. E. Dickinson, R. R. Nemani, Y. Knyazikhin, and R. B. Myneni, "Analysis of leaf area index products from combination of MODIS Terra and Aqua data," *Remote Sens. Environ.* **104**(3), 297–312 (2006). [doi:10.1016/j.rse.2006.04.016].

Downloaded from SPIE Digital Library on 18 Jan 2011 to 128.219.49.8. Terms of Use: http://spiedl.org/terms

[27] Q. Wang, J. Ni, and J. Tenhunen, "Application of a geographically-weighted regression analysis to estimate net primary production of chinese forest ecosystems," *Global Ecol. Biogeogr.* **14**(4), 379–393 (2005). [doi:10.1111/j.1466-822X.2005.00153.x].

[28] K. D. Kanniah, J. Beringer, L. B. Hutley, N. J. Tapper, and X. Zhu, "Evaluation of Collections 4 and 5 of the MODIS Gross Primary Productivity product and algorithm improvement at a tropical savanna site in northern Australia," *Remote Sens. Environ.* **113**(9), 1808–1822 (2009). [doi:doi:10.1016/j rse.2009.04.013].

[29] A. Verger, F. Baret, and M. Weiss, "Performances of neural networks for deriving LAI estimates from existing CYCLOPES and MODIS products," *Remote Sens. Environ.* **112**(6), 2789–2803 (2008). [doi:10.1016/j.rse.2008.01.006].

[30] L. M. Zhang, G. R. Yu, X. M. Sun, X. F. Wen, C. Y. Ren, Y. L. Fu, Q. K. Li, Z. Q. Li, Y. F. Liu, D. X. Guan, and J. H. Yan, "Seasonal variations of ecosystem apparent quantum yield (alpha) and maximum photosynthesis rate (P-max) of different forest ecosystems in China," *Agric. For. Meteorol.* **137**(3-4), 176–187 (2006). [doi:10.1016/j.agrformet.2006.02.006].

[31] R. Leuning, H. A. Cleugh, S. J. Zegelin, and D. Hughes, "Carbon and water fluxes over a temperate Eucalyptus forest and a tropical wet/dry savanna in Australia: measurements and comparison with MODIS remote sensing estimates," *Agric. For. Meteorol.* **129**(3-4), 151–173 (2005). [doi:10.1016/j.agrformet.2004.12.004].

[32] J. F. Xiao, Q. L. Zhuang, and D. Baldocchi et al., "Estimation of net ecosystem carbon exchange for the conterminous United States by combining MODIS and AmeriFlux data," *Agric. For. Meteorol.* **148**(11), 1827–1847 (2008). [doi:10.1016/j.agrformet.2008.06.015].

[33] S. Kang, S. W. Running, M. Zhao, J. S. Kimball, and J. Glassy, "Improving continuity of MODIS terrestrial photosynthesis products using an interpolation scheme for cloudy pixels," *Int. J. Remote Sens.* **26**(8), 1659–1676 (2005). [doi:10.1080/01431160512331326693].

[34] H. L. Fang, S. L. Liang, J. R. Townshend, and R. E. Dickinson, "Spatially and temporally continuous LAI data sets based on an integrated filtering method: Examples from North America," *Remote Sens. Environ.* **112**(1), 75–93 (2008). [doi:10.1016/j rse.2006.07.026].

[35] F. Gao, J. Morisette, R. Wolfe, G. Ederer, J. Pedelty, E. Masuoka, R. Myneni, B. Tan, and J. Nightingale, "An algorithm to produce temporally and spatially continuous MODIS-LAI time series," *IEEE Geosci. Remote Sens. Lett.* **5**(1), 60 (2008). [doi:10.1109/LGRS.2007.907971].

[36] E. Falge, D. Baldocchi, and R. Olson et al., "Gap filling strategies for defensible annual sums of net ecosystem exchange," *Agric. For. Meteorol.* **107**(1), 43–69 (2001). [doi:10.1016/S0168-1923(00)00225-2].

[37] W. P. Yuan, S. Liu, G. S. Zhou, G. Y. Zhou, L. L. Tieszen, D. Baldocchi, C. Bernhofer, H. Gholz, A. H. Goldstein, M. L. Goulden, D. Y. Hollinger, Y. Hu, B. E. Law, P. C. Stoy, T. Vesala, and S. C. Wofsy et al., "Deriving a light use efficiency model from eddy covariance flux data for predicting daily gross primary production across biomes," *Agric. For. Meteorol.* **143**(3-4), 189–207 (2007). [doi:10.1016/j.agrformet.2006.12.001].

[38] J. Grieser, R. Gommes, and M. Bernardi, "New LocClim-the Local Climate Estimator of FAO," in *Geophysical Research Abstracts*, **8**, 08305 (2006).

[39] H. McCarthy, R. Oren, A. Finzi, D. Ellsworth, H. Kim, K. Johnsen, and B. Millar, "Temporal dynamics and spatial variability in the enhancement of canopy leaf area under elevated atmospheric CO_2," *Global Change Biol.* **13**(12), 2479–2497 (2007). [doi:10.1111/j.1365-2486.2007.01455.x].

[40] H. R. McCarthy, R. Oren, H. S. Kim, K. H. Johnsen, C. Maier, S. G. Pritchard, and M. A. Davis, "Interaction of ice storms and management practices on current carbon sequestration in forests with potential mitigation under future CO_2 atmosphere," *J. Geophys. Res. Atmos.* **111**(D15), 10 (2006). [doi:10.1029/2005JD006428].

Downloaded from SPIE Digital Library on 18 Jan 2011 to 128.219.49.8. Terms of Use: http://spiedl.org/terms

[41] D. Y. Hollinger, S. M. Goltz, E. A. Davidson, J. T. Lee, K. Tu, and H. T. Valentine, "Seasonal patterns and environmental control of carbon dioxide and water vapour exchange in an ecotonal boreal forest," *Global Change Biol.* **5**(8), 891–902 (1999). [doi:10.1046/j.1365-2486.1999.00281.x].

[42] M. L. Goulden, G. C. Winston, A. M. S. McMillan, M. E. Litvak, E. L. Read, A. V. Rocha, and J. Rob Elliot, "An eddy covariance mesonet to measure the effect of forest age on land-atmosphere exchange," *Global Change Biol.* **12**(11), 2146–2162 (2006). [doi:10.1111/j.1365-2486.2006.01251.x].

[43] H. P. Schmid, C. S. B. Grimmond, F. Cropley, B. Offerle, and H. B. Su, "Measurements of CO_2 and energy fluxes over a mixed hardwood forest in the mid-western United States," *Agric. For. Meteorol.* **103**(4), 357–374 (2000). [doi:10.1016/S0168-1923(00)00140-4].

[44] L. K. Xu and D. D. Baldocchi, "Seasonal variation in carbon dioxide exchange over a Mediterranean annual grassland in California," *Agric. For. Meteorol.* **123**(1-2), 79–96 (2004). [doi:10.1016/j.agrformet.2003.10.004].

[45] L. B. Flanagan, L. A. Wever, and P. J. Carlson, "Seasonal and interannual variation in carbon dioxide exchange and carbon balance in a northern temperate grassland," *Global Change Biol.* **8**(7), 599–615 (2002). [doi:10.1046/j.1365-2486.2002.00491.x].

[46] A. Hyman, "Information presentation for new sensors: a focus on selected sensors of the Earth Observing System (EOS)," *Prog. Phys. Geog.* **20**(2), 146 (1996). [doi:10.1177/030913339602000202].

[47] Y. Knyazikhin, J. Glassy, J. L. Privette, Y. Tian, A. Lotsch, Y. Zhang, Y. Wang, J. T. Morisette, P. Votava, R. B. Myneni, R. R. Nemani, and S. W. Running, "MODIS Leaf Area Index (LAI) and Fraction of Photosynthetically Active Radiation Absorbed by Vegetation (FPAR) Product (MOD15) Algorithm Theoretical Basis Document." http://modis.gsfc nasa.gov/data/atbd/atbd_mod15.pdf (1999).

[48] Oak Ridge National Laboratory Distributed Active Archive Center (ORNL DAAC), Oak Ridge, Tennessee, U.S.A, "Modis subsetted land products, collection 5." (Accessed 08/24/2009) http://daac.ornl.gov/MODIS/modis html.

[49] M. Friedl, D. McIver, J. Hodges, X. Zhang, D. Muchoney, A. Strahler, C. Woodcock, S. Gopal, A. Schneider, A. Cooper, *et al.*, "Global land cover mapping from MODIS: algorithms and early results," *Remote Sens. Environ.* **83**(1), 287–302 (2002). [doi:10.1016/S0034-4257(02)00078-0].

[50] F. A. Heinsch, M. S. Zhao, and S. W. Running et al., "Evaluation of remote sensing based terrestrial productivity from MODIS using regional tower eddy flux network observations," *IEEE Trans. Geosci. Remote Sens.* **44**(7), 1908–1925 (2006). [doi:10.1109/TGRS.2005.853936].

[51] X. Chen, L. Vierling, D. Deering, and A. Conley, "Monitoring boreal forest leaf area index across a Siberian burn chronosequence: a MODIS validation study," *Int. J. Remote Sens.* **26**(24), 5433–5451 (2005). [doi:10.1109/TGRS.2005.853936].

[52] B. Tan, J. Hu, D. Huang, W. Yang, P. Zhang, N. Shabanov, Y. Knyazikhin, R. Nemani, and R. Myneni, "Assessment of the broadleaf crops leaf area index product from the Terra MODIS instrument," *Agric. For. Meteorol.* **135**(1-4), 124–134 (2005). [doi:10.1016/j.agrformet.2005.10.008].

[53] G. Bonan, *Ecological climatology: concepts and applications*, Cambridge University Press, Cambridge (2002).

[54] H. A. Cleugh, R. Leuning, Q. Mu, and S. W. Running, "Regional evaporation estimates from flux tower and MODIS satellite data," *Remote Sens. Environ.* **106**(3), 285 (2007). [doi:10.1016/j.rse.2006.07.007].

Downloaded from SPIE Digital Library on 18 Jan 2011 to 128.219.49.8. Terms of Use: http://spiedl.org/terms

[55] J. Demarty, F. Chevallier, A. Friend, N. Viovy, S. Piao, and P. Ciais, "Assimilation of global MODIS leaf area index retrievals within a terrestrial biosphere model," *Geophys. Res. Lett.* **34**(15), L15402 (2007). [doi:10.1029/2007GL030014].

[56] T. Chase, R. Pielke, T. Kittel, R. Nemani, and S. Running, "Sensitivity of a general circulation model to global changes in leaf area index," *J. Geophys. Res. D: Atmos.* **101**, 7393–7408 (1996). [doi:10.1029/95JD02417].

[57] J. Andersen, G. Dybkjaer, K. Jensen, J. Refsgaard, and K. Rasmussen, "Use of remotely sensed precipitation and leaf area index in a distributed hydrological model," *J. Hydrol.* **264**(1-4), 34–50 (2002). [doi:10.1016/S0022-1694(02)00046-X].

[58] J. Monteith, "Evaporation and surface temperature," *Q. J. R. Meteorolog. Soc.* **107**, 1–27 (1981). [doi:10.1256/smsqj.45101].

[59] A. Lindroth, "Aerodynamic and canopy resistance of short-rotation forest in relation to leaf area index and climate," *Boundary Layer Meteorol.* **66**(3), 265–279 (1993). [doi:10.1007/BF00705478].

[60] R. Leuning, Y. Zhang, A. Rajaud, H. Cleugh, and K. Tu, "A simple surface conductance model to estimate regional evaporation using MODIS leaf area index and the Penman-Monteith equation," *Water Resour. Res.* **44**(10), W10419 (2008). [doi:10.1029/2007WR006562].

[61] S. Franks, K. Beven, P. Quinn, and I. Wright, "On the sensitivity of soil-vegetation-atmosphere transfer (SVAT) schemes: equifinality and the problem of robust calibration," *Agric. For. Meteorol.* **86**(1-2), 63–75 (1997). [doi:10.1016/S0168-1923(96)02421-5].

[62] K. Schulz and K. Beven, "Data-supported robust parameterisations in land surface-atmosphere flux predictions: towards a top-down approach," *Hydrol. Processes* **17**(11), 2259–2277 (2003). [doi:10.1002/hyp.1331].

[63] M. Raupach, "Simplified expressions for vegetation roughness length and zero-plane displacement as functions of canopy height and area index," *Boundary Layer Meteorol.* **71**(1), 211–216 (1994). [doi:10.1007/BF00709229].

[64] W. Cohen, T. Maiersperger, D. Turner, W. Ritts, D. Pflugmacher, R. Kennedy, A. Kirschbaum, S. Running, M. Costa, and S. Gower, "MODIS land cover and LAI collection 4 product quality across nine sites in the western hemisphere," *IEEE Trans. Geosci. Remote Sens.* **44**(7), 1843–1857 (2006). [doi:10.1109/TGRS.2006.876026].

[65] M. Therezien, S. Palmroth, R. Brady, and R. Oren, "Estimation of light interception properties of conifer shoots by an improved photographic method and a 3D model of shoot structure," *Tree physiology* **27**(10), 1375 (2007). [doi:10.1093/treephys/27.10.1375].

[66] L. Wang, X. Xiong, J. Qu, Y. Xie, X. Hao, and N. Che, "Impact assessment of Aqua MODIS band-to-band misregistration on snow index," *J. Appl. Remote Sens.* **1**(013531) (2007). [doi:10.1117/1.2786934].

[67] K. Schulz, S. Franks, and K. Beven, "TOPUP - A TOPMODEL based SVAT model to calculate evaporative fluxes between the landsurface and the atmosphere." Version 1.1, Program Documentation.

[68] J. M. Barry, "SPLINS and SMOOTH: Two Fortran routines smoothing routines," tech. rep., Australian Atomic Energy Comission (AAEC), Research Establisment Lucas Heights (1973).

Downloaded from SPIE Digital Library on 18 Jan 2011 to 128.219.49.8. Terms of Use: http://spiedl.org/terms